Local microstructural analysis for $Y_2O_3/Eu^{3+}/Mg^{2+}$ nanorods by Raman and photoluminescence spectra under high pressure*

Jin-Hua Wang(王金华)[1,3], Ze-Peng Li(李泽朋)[2,3,†], Bo Liu(刘波)[3], and Bing-Bing Liu(刘冰冰)[3,‡]

[1] School of Science, Tianjin University of Technology and Education, Tianjin 300222, China
[2] School of Science, Civil Aviation University of China, Tianjin 300300, China
[3] State Key Laboratory of Superhard Materials, Jilin University, Changchun 130012, China

(Received 17 August 2016; revised manuscript received 28 October 2016; published online 20 December 2016)

In this paper, we investigate the Raman and photoluminescence spectra of Y_2O_3/Eu^{3+} and $Y_2O_3/Eu^{3+}/Mg^{2+}$ nanorods under high pressures using 514-nm and 532-nm laser light excitation. We observe transitions from the initial cubic phase to amorphous at pressures higher than 24 GPa for both Y_2O_3/Eu^{3+} and $Y_2O_3/Eu^{3+}/Mg^{2+}$ nanorods. In addition, Y_2O_3/Eu^{3+} and $Y_2O_3/Eu^{3+}/Mg^{2+}$ nanorods exhibit different distorted states after the pressure has been raised to 8 GPa. The analyses of intensity ratios, I_{0-2}/I_{0-1} from $^5D_0$–$^7F_2$ to $^5D_0$–$^7F_1$ and $I_{0-2}A/B$ of $^5D_0$–$^7F_2$ transitions indicate that $Y_2O_3/Eu^{3+}/Mg^{2+}$ nanorods exhibit stronger local micro-surrounding characteristics for Eu^{3+} ions in a pressure-modulated crystal field. The doped Mg^{2+} ion results in reducing the crystal ionicity in the distorted lattice state under high pressures. The use of doped ions as an ion modifier can be applied to the study of small local microstructural changes through Eu^{3+} luminescence.

Keywords: high-pressure, Y_2O_3/Eu^{3+},local structure

PACS: 61.46.Km, 78.55.Qr **DOI:** 10.1088/1674-1056/26/2/026101

1. Introduction

Rare-earth (RE)-doped nanomaterials possess extensive applications in lasers, three-dimensional (3D) display devices, optical temperature sensors, and optical amplifiers due to their excellent luminescence properties.[1–3] Consequently, the design and application of RE-doped nanomaterial is currently a field which the researchers are greatly interested in, focusing on gaining a better understanding of their properties. Numerous methods have been successfully used to improve the optical properties of RE-doped nanomaterials.[4–6] For example, ion doping has been demonstrated to be able to change the luminescence properties by modulating lattice fields and influencing the energy transfer behavior. For instance, Eu^{3+}-doped Y_2O_3 nanomaterials are used widely as RE-doped nanomaterials in several applications, particularly in display fields.[7–10] In terms of its optical property applications, slight changes in the crystal field environment have been shown to play an important role, with the exception of influences due to variations in dopant and doping amount.[11–13] Doped Eu^{3+} ions exist in the yttrium oxide (Y_2O_3) host in small quantities, with the energy transfer between Eu^{3+} ions and Y_2O_3 host being sensitive to the surrounding local microenvironment in addition to the crystal environment.[14–17]

High pressure has been demonstrated to be an effective method to induce significant changes in the structure and properties of materials. Under pressure, materials undergo lattice compression. This causes further potential structural transitions to occur, which can induce changes in the properties or lattice behavior of the material.[18–21] In the case of Y_2O_3 (Eu^{3+}) nanomaterial, pressure-induced microstructural deformation ahead of the lattice amorphous transition results in completely distinct microstructural states for doping Eu^{3+} ions.[22] This clearly results in a change in crystal environment, which subsequently changes the local environment of Eu^{3+} ions. In addition, other doping ions cause a nonhomogeneous distortion of the microstructure, which is amplified under high pressure due to lattice compression. Thus, using high-pressure is a useful method of understanding the influence of the crystal environment and the local surroundings on luminescence behavior. Therefore, the studies of the pressure-dependent luminescence of Y_2O_3/Eu^{3+} nanomaterials assisted by doping ion modulation could provide valuable insights for the field.

Numerous studies have demonstrated the luminescence properties of Eu^{3+} ions under high pressure. However, few studies have focused on lattice microstructural behavior under induced pressure as a result of changes in crystal environments and local micro-surrounding with other doping ions.[19,23–28] Investigations aiming to study the pressure-dependent photoluminescence (PL) spectra of both Y_2O_3/Eu^{3+} bulk and nano-

*Project supported by the National Natural Science Foundation of China (Grant Nos. 11304380, 11404241, 11275138, 11604240, and 51320105007) and the Program for Changjiang Scholars and Innovative Research Team in University, China (Grant No. IRT1132).

†Corresponding author. E-mail: li_zepeng@163.com
‡Corresponding author. E-mail: liubb@jlu.edu.cn

© 2017 Chinese Physical Society and IOP Publishing Ltd

materials by using either 514.5-nm or 532-nm laser excitation reported red spectral shifts and a loss of PL peaks.[20,22–28] In our recent study, we demonstrated the probe effect of up-conversion PL measurement in revealing slight changes of YO_6 octahedron in Y_2O_3/Eu^{3+} nanotubes under high pressure.[19] However, currently, there are no studies to analyze the pressure behavior of the luminescence of Y_2O_3/Eu^{3+} nanomaterials by manipulating other auxiliary ions under high pressure. The study of microstructure-related luminescence properties would provide important insights into the understanding of the luminescence behavior of Eu^{3+} ions and ways to utilize Eu^{3+}-doped Y_2O_3 nanomaterials.

In the present work, we carry out high-pressure experiments to investigate local microstructures through Raman and PL spectra of Y_2O_3/Eu^{3+} and $Y_2O_3/Eu^{3+}/Mg^{2+}$ nanorods by using 514-nm and 532-nm laser excitation. The amorphous transitions are found to occur at a pressure greater than 24 GPa for both Y_2O_3/Eu^{3+} and $Y_2O_3/Eu^{3+}/Mg^{2+}$ nanorods. Under high pressure (above 8 GPa), Y_2O_3/Eu^{3+} and $Y_2O_3/Eu^{3+}/Mg^{2+}$ nanorods exhibit different distorted states. In addition, Y_2O_3/Eu^{3+} and $Y_2O_3/Eu^{3+}/Mg^{2+}$ nanorods present different local micro-surrounding characteristics for Eu^{3+} ion in a pressure-modulated crystal field, based on the analyses of the following intensity ratios: I_{0-2}/I_{0-1} of $^5D_0$–$^7F_2$ to $^5D_0$–$^7F_1$ and $I_{0-2}A/B$ of $^5D_0$–$^7F_2$ transitions. The doped Mg^{2+} ion is found to play a critical role in reducing the local microstructure ionicity when the YO_6 octahedron is distorted under high pressure. From this work, we show that doped ions can be utilized for detecting the tiny local microstructural changes upon high pressure by using Eu^{3+} luminescence.

2. Experimental details

The Y_2O_3/Eu^{3+} and Mg^{2+} co-doped Y_2O_3/Eu^{3+} nanorods used in this study were generated using a hydrothermal method as described previously.[29] The Eu^{3+} doped $Y_{1.9}Eu_{0.1}O_3$ (YEO) and Mg^{2+} co-doped $Y_{1.8}Eu_{0.1}Mg_{0.1}O_3$ (YEMO) samples were placed in a cubic structure (space group: *Ia*-3) and comprised of nanorods that were predominantly 50 nm–100 nm in diameter and 10 μm in length as depicted in Fig. 1. A diamond anvil cell (DAC) was used to carry out Raman and PL spectra experiments under high pressure. These experiments were done by using a 4:1 methanol–ethanol mixture as pressure medium. The pressure was calibrated by a shift in the ruby R_1 line. A Renishaw inVia Raman Microscope equipped with a charge coupled device (CCD) detector was used to collect Raman vibrational signals from 514.5-nm excitation. A spectrometer (focal length, 500 mm) combined with a liquid nitrogen-cooled CCD (Acton SP-2500 and PyLoN:100B, Princeton Instruments) was utilized to obtain high-pressure PL spectra. A 532-nm single-mode diode-pumped solid-state (DPSS) laser (power output, 50 mW) was used as the light source for experiments by using PL excitation. In PL experiments, all data were collected under identical experimental conditions for each pressure tested, including the same laser power, laser spot size, exposure time, and focus microscopic lens. The spectra resolutions are 1 cm^{-1} and 0.1 nm, respectively for Raman and luminescence spectrometers in the high pressure experiments carried out in this study.

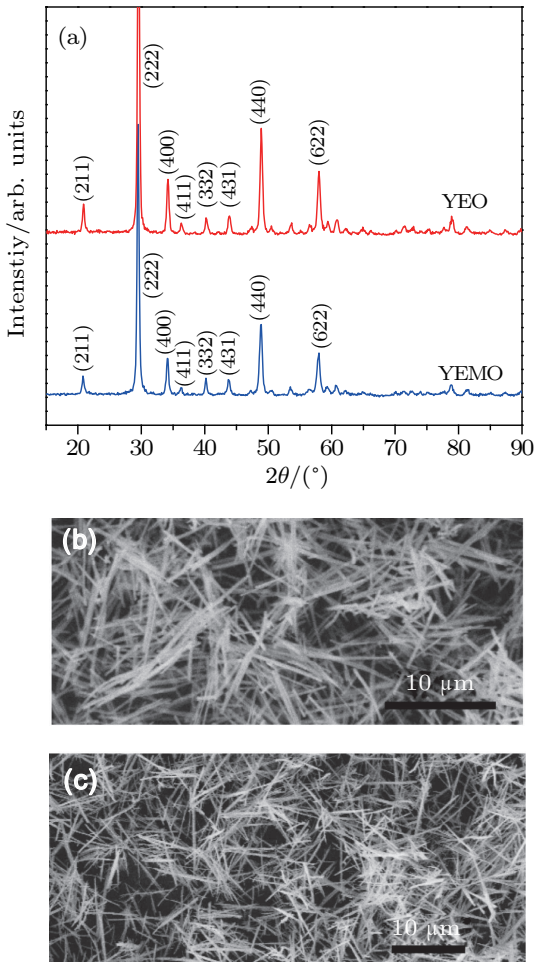


Fig. 1. (color online) X-ray diffraction (XRD) patterns (a) and SEM images of YEO (b) and YEMO (c) nanorods in ambient conditions.

3. Results and discussion

Figure 2 illustrates the PL spectra in a range of 550 nm–675 nm ($^5D_0$–$^7F_{0,1,2}$) of YEO and YEMO nanorods under ambient conditions by using a laser excitation of 532 nm. With laser excitation, energy transfers to Eu^{3+} ions via the Y_2O_3 host lattice. Energy transfer is a critical determinant of the PL behavior of RE-doped material, and this energy transfer behavior is dependent on the structure and local microstructure of Eu^{3+} ions. Therefore, the study of pressure-dependent PL of Eu^{3+} ions could provide valuable insights into the changes in structural and local microstructural behavior, and also the changes in corresponding relationship between the Eu^{3+} ion PL and local microstructure.

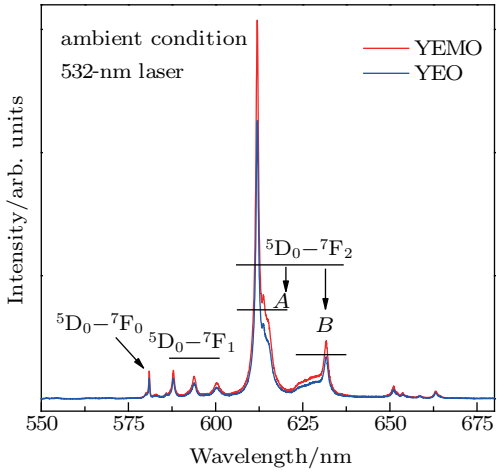


Fig. 2. (color online) Photoluminescence spectra of $Y_{1.9}Eu_{0.1}O_3$ (YEO) and Mg^{2+} co-doped $Y_{1.8}Eu_{0.1}Mg_{0.1}O_3$ (YEMO) nanorods under ambient conditions.

In order to characterize structural changes, we carry out *in-situ* Raman scattering experiments on YEO and YEMO nanorods and show the pressure-dependent Raman spectra in Fig. 3. The representative Raman vibration of Y^{3+}–O^{-2} located at 378 cm^{-1} in ambient conditions is observed to shift towards high wave numbers with increasing pressure. The intensity of the Raman vibration is observed to become notably weaker after 8 GPa–9 GPa, in the cases of YEO and YEMO samples. For YEO nanorods, the Raman vibration becomes very weak when the pressure reaches up to 18.9 GPa, and disappears completely at 24.2 GPa. Similar results were observed for YEMO nanorods, in which the Raman vibration begins to disappear when the pressure reaches up to 20 GPa. The disappearances of the Raman vibration for both YEO and YEMO nanorods indicate a phase transition from initial cubic structure to a different structure. With increasing pressure, no distinguishable Raman signal is detected. The phase transition behavior observed for Y_2O_3/Eu^{3+} nanomaterials doped with Eu^{3+} or Mg^{2+} ion(s) is similar to that of its Y_2O_3host, with Y_2O_3 and Y_2O_3/Eu^{3+} nanomaterials reported to transform from an initial cubic phase into an amorphous phase.[14,15,20,24] In addition to the disappearance of the Raman vibration, the Raman peak position is also observed to shift towards a higher wavenumber as deduced by pressure treatment. However, the Raman peak position is found to shift at different rates under pressure prior to the amorphous transition at 24 GPa. This observation is ascribed to the pressure-induced YO_6 octahedron distortion.[22] We plot the pressure-dependent Raman peak position in Fig. 4. These plots show different variations of Raman vibration before and after 8 GPa of pressure: the peak shift becomes slower after 8 GPa and has an obvious change in the slope. This illustrates that the Raman peak shift that occurs with pressure induced by lattice compression becomes slower after 8 GPa. Below approximately 8 GPa, the variations in the Raman vibration are found to be consistent for YEO and YEMO nanorods. However, the changes in the extent of the slope become different after 8 GPa, with the slope changing less markedly in the case of YEMO nanorods. As previously reported, the different changes in behavior of the Raman vibration slope under pressure correspond to different lattice states that exist before structure transformation.[22] The latter lattice state is thought of as a slightly distorted state that results from the YO_6 octahedron distortion. The weakened Raman intensity mentioned previously is caused by a local distortion of the Y_2O_3 lattice. In the present study, we show that the difference in distortion state between YEO and YEMO nanorods is mainly due to Mg^{2+} doping into the Y_2O_3 lattice, which generates a different pressure behavior for the YO_6 deformation.

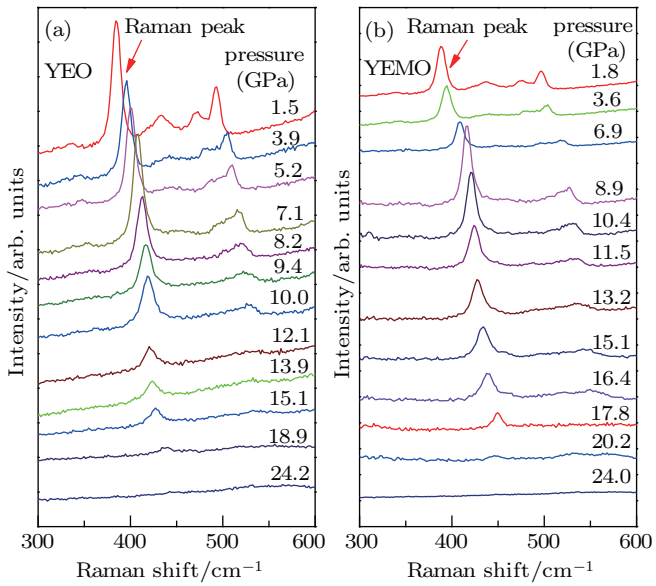


Fig. 3. (color online) Pressure-dependent Raman spectra of YEO and YEMO nanorods.

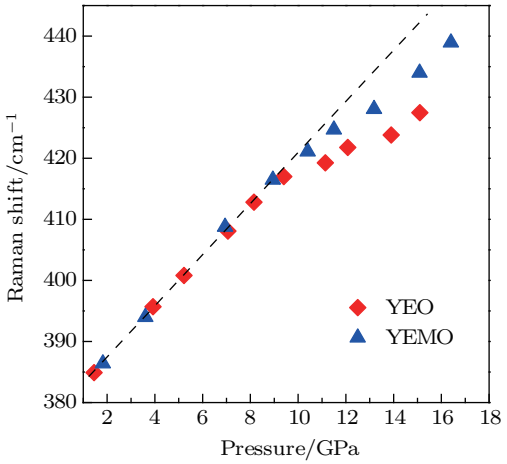


Fig. 4. (color online) Raman peak positions of YEO and YEMO nanorods under high pressure.

The different lattice states of YEO and YEMO nanorods correspond to different crystal fields, which play a critical role in determining the luminescence properties of the doping Eu^{3+} ion. Thus, we successively analyze the pressure-dependent PL

experiments of YEO and YEMO nanorods excited with a 532-nm laser. Given that $^5D_0$–$^7F_{0,1,2}$ transitions exhibit comparatively strong PL intensities and reflect the information about crystal fields and local microstructural changes, we analyze the pressure-dependent PL spectra of $^5D_0$–$^7F_{0,1,2}$ transitions for both YEO and YEMO nanorods (Fig. 5).

With increasing pressure, all $^5D_0$–$^7F_{0,1,2}$ transition peaks are found to shift towards higher wavelengths with a lattice compression. The strongest peak at 612 nm in ambient conditions becomes definitively weaker after 8 GPa, in the cases of both YEO and YEMO nanorods. When the pressure reaches up to 23 GPa–24 GPa, the group A peaks from the $^5D_0$–$^7F_2$ transition (indicated in Fig. 2) are found to become weak, and therefore difficult to distinguish. This could be attributed to the amorphous transition of the Y_2O_3 host lattice that occurs under high pressure. Given the transition sensitivity of the Eu^{3+} ion to the local structure of the Y_2O_3 lattice, studies into factors that influence local structural changes on the PL spectra can provide valuable information. Corresponding changes in the local microstructure can be explained by the Judd–Ofelt theory.[30,31] The Judd–Ofelt parameter Ω_2, defined as the intensity ratio I_{0-2}/I_{0-1} of $^5D_0$–$^7F_2$ to $^5D_0$–$^7F_1$ transitions of Eu^{3+} ions, is related to short-range effect and reflects the properties of the local microstructure and surrounding Eu^{3+} ions. Meanwhile, the intensity ratio $I_{0-2}A/B$ of $^5D_0$–$^7F_2$ transitions also reflects a similar behavior of the lattice microstructural information.[28]

We plot the intensity ratios I_{0-2}/I_{0-1} and $I_{0-2}A/B$ of $^5D_0$–$^7F_2$ transitions of Eu^{3+} ions against pressure in Figs. 5 and 6. The intensity ratio I_{0-2}/I_{0-1} exhibits different changes in behavior under pressures both below and above 8 GPa, while $I_{0-2}(A/B)$ exhibits a sudden drop around 8 GPa. The I_{0-2}/I_{0-1} ratio is observed to increase with pressure before 8 GPa, and decrease rapidly after 8 GPa. As discussed previously, an amorphous transition of the Y_2O_3 host lattice occurs at pressures higher than 20 GPa. Therefore, the sudden change observed in the I_{0-2}/I_{0-1} ratio around 8 GPa is not caused naturally by the structural transition. This sudden change could be attributed to local structural changes of the YEO and YEMO nanorods. As Raman vibration under pressure indicates, the vibration position of the typical Raman mode Y^{3+}–O^{-2} is found to increase at different rates before and after 8 GPa. This demonstrates that the micro-surrounding of Eu^{3+} ions clearly changes. Before 8 GPa, the I_{0-2}/I_{0-1} ratio is found to increase, indicating a crystal field strengthening for both YEO and YEMO nanorods. Indeed, the pressure causes a decrease in the distance between atoms and shortens bond lengths, which could ultimately result in the strengthening of the crystal field. After 8 GPa, the Y_2O_3 host lattice is found to transform into a distorted state in some local microstructures. However, the structure transformation is shown not to occur for the Y_2O_3 host lattice as illustrated by the Raman study. This transformation induces the crystal microstructure to change, followed by direct influence on the surrounding Eu^{3+} ions. In this disordered lattice state, the general lattice space is shown to be compressed continuously with pressure. However, the local microstructural disorder destroys the strengthening tendency of the Eu^{3+} local micro-surroundings. Under such circumstances, the covalency in the vicinity of Eu^{3+} ion-ligand increases, and the ionicity of Eu^{3+} local micro-surroundings exhibits a corresponding decrease.[30,31] Therefore, the intensity ratio I_{0-2}/I_{0-1} is found to decrease after 8 GPa, with the degree of decrease becoming larger with distortion increasing under pressure.

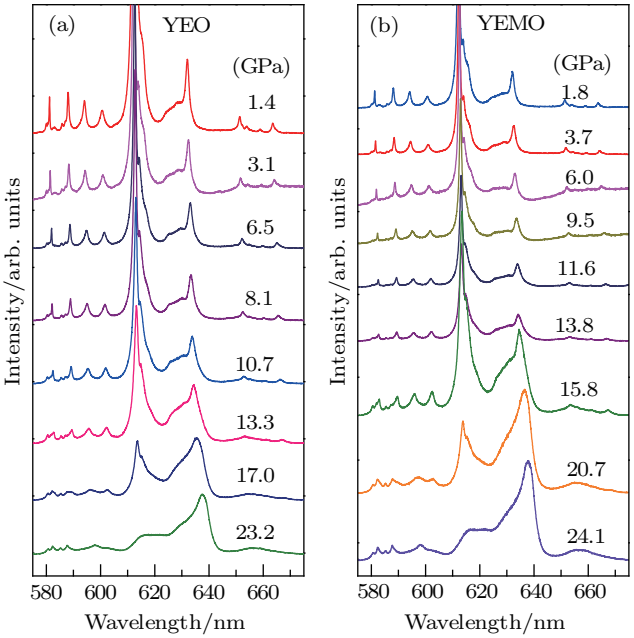


Fig. 5. (color online) Pressure-dependent PL spectra of YEO and YEMO nanorods.

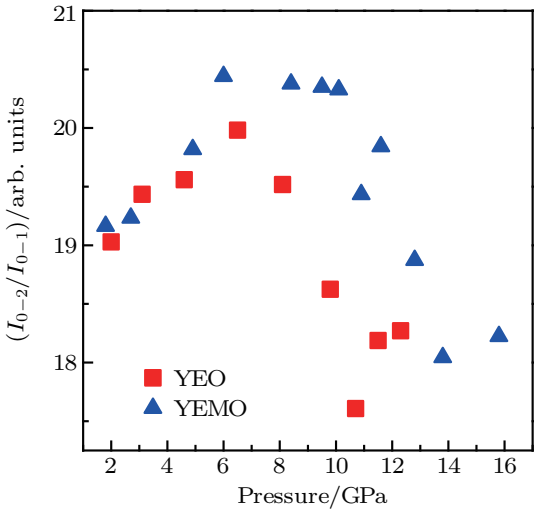


Fig. 6. (color online) PL intensity ratios I_{0-2}/I_{0-1} of $^5D_0$–$^7F_2$ and $^5D_0$–$^7F_1$ transitions of YEO and YEMO nanorods with increasing pressure.

In addition to the sudden changes in intensity ratios of I_{0-2}/I_{0-1} and $I_{0-2}A/B$ around 8 GPa, we also observe that

there is no typical Raman vibration position nor intensity ratio (I_{0-2}/I_{0-1} and $I_{0-2}A/B$), which shows a different sudden change degree for each of YEO and YEMO nanorods. This suggests that both YEO and YEMO nanorods exhibit different crystal field properties and local micro-surroundings of Eu^{3+} ions after 8 GPa. As shown in Figs. 6 and 7, YEMO nanorods display higher intensity ratios of I_{0-2}/I_{0-1} and $I_{0-2}A/B$ at each pressure point measured after 8 GPa, which indicates that according to the Judd–Ofelt theory,[30] the ionicity of the Eu^{3+} local micro-surroundings for YEMO nanorods is greater than that of YEO nanorods, although they are both in distorted lattice states. In the pressure-dependent Raman vibration spectra under high pressure, we also demonstrate that the vibration position variation differs after 8 GPa, with the larger bend observed with YEO nanorods, and the smaller bend observed with YEMO nanorods. Therefore, the different bend degrees of the Raman mode variety and intensity ratios (I_{0-2}/I_{0-1} and $I_{0-2}A/B$) observed under high pressures appearing at 8 GPa are consistent and closely related to each other. As the pressure-dependent Raman studies illustrate, different bends indicate different distortion states in the local microstructure, with the smaller bend degree of Raman vibration exhibiting the weak distortion of the YO_6 octahedron for YEMO nanorods under high pressure. This leads to the higher ionicity of the local microstructure, corresponding to the higher ionicity of Eu^{3+} local micro-surroundings. Therefore, the intensity ratios, I_{0-2}/I_{0-1} of $^5D_0$–$^7F_2$ to $^5D_0$–$^7F_1$ and $I_{0-2}A/B$ of $^5D_0$–$^7F_2$ transitions, exhibit higher values under high pressure in the case of Mg^{2+} co-doped YEMO nanorods.

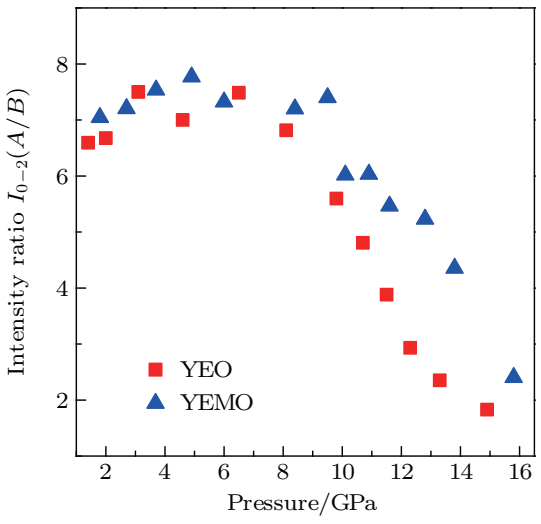


Fig. 7. (color online) PL intensity ratios $I_{0-2}A/B$ of $^5D_0$–$^7F_2$ transitions of YEO and YEMO nanorods with increasing pressure.

The doped Mg^{2+} ions act as modifiers of the Y_2O_3 lattice and YO_6 octahedron. These doped Mg^{2+} ions are believed to play a critical role in modifying the microstructure and local micro-surroundings of Eu^{3+}.[32] Compared with the radii of Y^{3+} (0.089 nm) and Eu^{3+} (0.198 nm) ions, the ionic radius of Mg^{2+} is small (0.072 nm). Following doping, the doped Mg^{2+} ions partially substitute the Y^{3+}. The Mg^{2+} ion modification shortens the Mg–O bond length, compared with the undoped Y–O bond length. Due to the microscaled doping of Mg^{2+}, the Y_2O_3 host lattice does not exhibit general structural changes in ambient conditions in the lower pressure range. However, when the pressure is greater than 8 GPa, the $Y_2O_3(Y_2O_3/Eu^{3+})$ host lattice transforms into a distorted state, deforming the YO_6 octahedron. Consequently, the doping effects of Mg^{2+} ions on the Y_2O_3 crystal lattice become clear. According to the results from a previous study, the two different kinds of YO_6 octahedrons of $Y_2O_3(Y_2O_3/Eu^{3+})$ nanomaterials exhibit different deformation properties.[14] The YO_6 octahedron with C_2 symmetry is demonstrated to be easily distorted by pressure compared with the octahedron with S_6 symmetry. Due to the fact that the YO_6 octahedron becomes distorted under pressures greater than 8 GPa, ideal $Y_2O_3(Y_2O_3/Eu^{3+})$, the lattice arrangement breaks, inducing a decrease in the local microstructure ionicity. Thus, the intensity ratios, I_{0-2}/I_{0-1} of $^5D_0$–$^7F_2$ to $^5D_0$–$^7F_1$ and $I_{0-2}A/B$ of $^5D_0$–$^7F_2$ transitions of Eu^{3+} are found to exhibit a sudden drop with pressure increasing. In the case of the Mg^{2+}-ion-doped $Y_2O_3(Y_2O_3/Eu^{3+})$, the decrease in the $Y_2O_3(Y_2O_3/Eu^{3+})$ microstructure ionicity is found to be attenuated due to its shorter Mg–O bond length, which is found to strengthen the crystal field. Therefore, the YEMO nanorods show higher intensity ratios of I_{0-2}/I_{0-1} of $^5D_0$–$^7F_2$ to $^5D_0$–$^7F_1$ and $I_{0-2}A/B$ of $^5D_0$–$^7F_2$ transitions. This suggests that the doped ions can be used as a lattice ion modifier to study tiny local microstructural changes induced through Eu^{3+} luminescence under high pressure.

4. Conclusions

In this work, we perform pressure-induced microstructural analyses of Y_2O_3/Eu^{3+} and $Y_2O_3/Eu^{3+}/Mg^{2+}$ nanorods using Raman and photoluminescence spectra. The Y_2O_3/Eu^{3+} and $Y_2O_3/Eu^{3+}/Mg^{2+}$ nanorods are shown to transform into an amorphous phase at a pressure of 24 GPa. Pressure-dependent Raman peak positions exhibit different distorted states after 8 GPa, in the cases of Y_2O_3/Eu^{3+} and $Y_2O_3/Eu^{3+}/Mg^{2+}$ nanorods. The $Y_2O_3/Eu^{3+}/Mg^{2+}$ nanorods are demonstrated to exhibit a stronger crystal field around Eu^{3+} ions when the intensity ratios of I_{0-2}/I_{0-1} of $^5D_0$–$^7F_2$ to $^5D_0$–$^7F_1$ and $I_{0-2}A/B$ of $^5D_0$–$^7F_2$ transitions in the distorted lattice state are investigated. The doped Mg^{2+} ion is found to play a critical role in reducing the decrease in crystal ionicity under high pressure. Additionally, these studies show that the doped ions can be used as a lattice ion modifier to investigate tiny local microstructural changes with the help of Eu^{3+} luminescence under high pressure.

References

[1] Perrot A, Goldner P, Giaume D, Lovric M, Andriamiadamanana C, Goncalves R R and Ferrier A 2013 *Phys. Rev. Lett.* **111** 203601

[2] Xu S, Xu W, Wang Y F, Zhang S, Zhu Y S, Tao L, Xia L, Zhou P W and Song H W 2014 *Nanoscale* **6** 5859

[3] Sun T P, Zhang D Q, Yu X F, Xiang Y, Luo M, Wang J H, Tan G L, Wang Q Q and Chu P K 2013 *Nanoscale* **5** 1629

[4] Liu J P, Li Y Y, Huang X T, Li Z K, Li G Y and Zeng H B 2008 *Chem. Mater.* **20** 250

[5] Chen G Y, Zhang Y G, Somesfalean G, Zhang Z G, Sun Q and Wang F P 2006 *Appl. Phys. Lett.* **89** 163105

[6] Yu M, Lin J, Wang Z, Fu J, Wang S, Zhang H J and Han Y C 2002 *Chem. Mater.* **14** 2224

[7] Kasperczyk M, Person S, Ananias D, Carlos L D and Novotny L 2015 *Phys. Rev. Lett.* **114** 163903

[8] Jadhav A P, Kim C W, Cha H G, Pawar A U, Jadhav N A, Pal U and Kang Y S 2009 *J . Phys. Chem. C* **113** 13600

[9] Cui H, Zhu P F, Zhu H Y, Li H D and Cui Q L 2014 *Chin. Phys. B* **23** 057801

[10] Shi H, Zhang X Y, Dong W L, Mi X Y, Wang N L, Li Y and Liu H W 2016 *Chin. Phys. B* **25** 047802

[11] Paez D Y 2016 *Polyhedron* **105** 35

[12] Sarakovskis A, Krieke G, Doke G, Grube J, Grinberga L and Springis M 2015 *Opt. Mater.* **39** 90

[13] Dondi M, Ardit M, Cruciani G and Zanelli C 2014 *Am. Mineral.* **99** 1736

[14] Li Z P, Wang J H, Wang L, Bai X, Song H W, Zhou Q J, Wei T, An D M and Liu B B 2014 *Mater. Res. Express* **1** 025013

[15] Li Z P, Wang J H, Hou Y Y, Bai X, Song H W, Zhou Q J, Wei T, Li Y and Liu B B 2015 *RSC Adv.* **5** 3130

[16] Wu X W, Wu D J and Liu X J 2009 *Chin. Phys. Lett.* **26** 077809

[17] Wang Y, Wu D D, Yang Y T and Liu X J 2011 *Chin. Phys. Lett.* **28** 027804

[18] Sato T and Funamori N 2008 *Phys. Rev. Lett.* **101** 255502

[19] Swamy V, Kuznetsov A, Dubrovinsky L S, McMillan P F, Prakapenka V B, Shen G and Muddle B C 2006 *Phys. Rev. Lett.* **96** 135702

[20] Wang L, Yang W, Ding Y, Ren Y, Xiao S, Liu B, Sinogeikin S V, Meng Y, Gosztola D J, Shen G, Hemley R J, Mao W L and Mao H K 2010 *Phys. Rev Lett.* **105** 095701

[21] Li C, Arfan B, Shen X, Kong P P, Wang W P, Zhao H F, Yao Y, Zou B S, Li Y C, Li X D, Liu J, Jin C Q and Yu R C 2015 *Chin. Phys. B* **24** 036401

[22] Li Z P, Xu H, Liu B, Song Q G, Zhou Q J, Song H W and Liu B B 2016 *Phys. Status Solidi B* **253** 2204

[23] Wang L, Pan Y X, Ding Y, Yang W G, Mao W L, Sinogeikin S V, Meng Y, Shen G Y and Mao H K 2009 *Appl. Phys. Lett.* **94** 061921

[24] Zhu H Y, Ma Y Z, Yang H B, Zhu P F, Du J G, Ji C and Hou D B 2010 *Solid State Commun.* **150** 1208

[25] Dai R C, Zhang Z M, Zhang C C and Ding Z 2010 *J. Nanosci. Nanotech.* **10** 7629

[26] Bai X, Song H W, Liu B B, Hou Y Y, Pan G H and Ren X G 2008 *J. Nanosci. Nanotechol.* **8** 1404

[27] Dai R C, Wang Z P, Zhang Z M and Ding Z J 2010 *J. Rare Earths* **28** 241

[28] Zhang J, Cui H, Zhu P F, Ma C L, Wu X X, Zhu H Y, Ma Y Z and Cui Q L 2014 *J. Appl. Phys.* **115** 023502

[29] Liu Z L, Yu L X, Wang Q, Tao Y C and Yang H 2011 *J. Lumin.* **131** 12

[30] Judd B R 1962 *Phys. Rev.* **127** 750

[31] Ofeit G S 1962 *J. Chem. Phys.* **37** 511

[32] Capobianco J A, Proulx P P, Bettinelli M and Negrisolo F 1990 *Phys. Rev. B* **42** 5936